

Convergence of Newton's Method for a Minimization Problem in Impulse Noise Removal

Raymond H. Chan, Chung-Wa Ho^{*} and Mila Nikolova[†]

February 5, 2004

Abstract

Recently, two-phase schemes for removing salt-and-pepper and random-valued impulse noise are proposed in [6, 7]. The first phase uses decision-based median filters to locate those pixels which are likely to be corrupted by noise (noise candidates). In the second phase, these noise candidates are restored using a detail-preserving regularization method which allows edges and noise-free pixels to be preserved. As shown in [18], this phase is equivalent to solving a one-dimensional nonlinear equation for each noise candidate. One can solve these equations by using Newton's method. However, because of the edge-preserving term, the domain of convergence of Newton's method will be very narrow. In this paper, we determine the initial guesses for these equations such that Newton's method will always converge.

1 Introduction

Impulse noise is caused by malfunctioning pixels in camera sensors, faulty memory locations in hardware, or transmission in a noisy channel. Some of the pixels in the images could be corrupted by the impulse noise while the remaining pixels remain unchanged. There are two types of impulse noise: fixed-valued noise and random-valued noise. For images corrupted by fixed-valued noise, the noisy pixels can take only some of the values in the dynamic range, e.g. the maximum and the minimum values in the so-called salt-and-pepper noise model. In contrast, the noisy pixels in images corrupted by random-valued noise can take any random values in the dynamic range.

There are many works proposed to clean the noise, see for instance the schemes proposed in [2, 17, 1, 12, 13, 19, 18, 6, 7]. In particular, decision-based median filters are popular in removing impulse noise because of their good denoising power and computational efficiency, see [16, 15, 22, 9, 20, 14]. However, the blurring of details and edges are clearly visible when the noise level is high. In comparison, the detail-preserving variational method proposed in [18] used non-smooth data-fitting term along with edge-preserving regularization to restore the images. The variational method can keep the edges. But when removing noise patches—several noise pixels connecting each other, the distortion of some uncorrupted image pixels at the edges cannot be avoided. To overcome the drawbacks, the two-phase schemes recently proposed in [6, 7] combine decision-based median filters and the detail-preserving variational method to clean the noise.

The first phase in the methods proposed in [6, 7] is based on the adaptive median filter [15] or the adaptive center-weighted median filter [9] to first locate those pixels which are likely to be corrupted by noise (noise candidates). Because of computational efficiency of median filters, this phase can be processed in a short time. The second phase is to restore those noise candidates by variational method

^{*}R. H. Chan and C. W. Ho are with the Department of Mathematics, The Chinese University of Hong Kong, Shatin, Hong Kong (email: {rchan, cwho}@math.cuhk.edu.hk). This work was supported by HKRGC Grant and CUHK DAG.

[†]M. Nikolova is with the Centre de Mathématiques et de Leurs Applications (CMLA - CNRS UMR 8536), ENS de Cachan, 61 av. du President Wilson, 94235 Cachan Cedex, France (email: nikolova@cmla.ens-cachan.fr).

given in [18]. It is to minimize the objective functional consisting of a data-fitting term and an edge-preserving regularization term. It is equivalent to solving a system of nonlinear equations for those noise candidates. As shown in [18], the root finding can be done by relaxation, and it results in solving a one-dimensional nonlinear equation for each noise candidate. The presence of the edge-preserving regularization term introduces difficulties in solving the equations because the nonlinear functions can have very large derivatives in some regions. In particular, the convergence domain can be very small if Newton's method is used. In this report, we give an algorithm to locate the initial guess such that Newton's method always converges.

The outline of this report is as follows. In §2, we review both two-phase denoising schemes proposed in [6] and [7] for cleaning impulse noises. The initial guess of Newton's method for solving nonlinear equations is discussed in §3. Numerical results and conclusions are presented in §4 and §5 respectively.

2 Review of 2-Phase Denoising Schemes

Let $\{x_{ij}\}_{i,j=1}^{M,N}$ be the gray level of a true image \mathbf{x} at pixel location (i, j) , and $[s_{\min}, s_{\max}]$ be the dynamic range of \mathbf{x} . Denote \mathbf{y} the noisy image. The observed gray level at pixel location (i, j) is given by

$$y_{ij} = \begin{cases} r_{ij}, & \text{with probability } p, \\ x_{ij}, & \text{with probability } 1 - p, \end{cases}$$

where p defines the noise level. In salt-and-pepper noise model, r_{ij} take either s_{\min} or s_{\max} , i.e. $r_{ij} \in \{s_{\min}, s_{\max}\}$, see [15]. In random-valued noise model, $r_{ij} \in [s_{\min}, s_{\max}]$ are random numbers, see [9].

2.1 Cleaning salt-and-pepper noise

A two-phase scheme is proposed in [6] to remove salt-and-pepper noise. The first phase is to use the adaptive median filter (AMF) [15] to identify the noise candidates. Then the second phase is to restore those noise candidates by minimizing the objective functional proposed in [18] which consists of an ℓ_1 data-fitting term and an edge-preserving regularization term. The algorithm is as follows:

Algorithm I

1. (*Noise detection*): Apply AMF to the noisy image \mathbf{y} to get the noise candidate set \mathcal{N} .
2. (*Refinement*): If the range of the noise is known, we can refine \mathcal{N} to \mathcal{N}_T . For example,

$$\mathcal{N}_T = \mathcal{N} \cap \{(i, j) : s_{\min} \leq y_{ij} \leq s_{\min} + T \quad \text{or} \quad s_{\max} - T \leq y_{ij} \leq s_{\max}\},$$

where $T \geq 0$ is a threshold. Or we can choose T such that

$$\frac{|\mathcal{N}_T|}{M \times N} \approx p.$$

In the case of salt-and-pepper noise we can take T close to zero.

3. (*Restoration*): We restore all pixels in \mathcal{N}_T by minimizing the convex objective functional $F_{\mathbf{y}}$:

$$\begin{aligned} F_{\mathbf{y}}(\mathbf{x}) = & \sum_{(i,j) \in \mathcal{N}_T} |x_{ij} - y_{ij}| + \frac{\beta}{2} \left(\sum_{(i,j) \in \mathcal{N}_T} \sum_{(m,n) \in \mathcal{V}_{ij}} \varphi_{\alpha}(x_{ij} - x_{mn}) \right. \\ & \left. + \sum_{(m,n) \in \mathcal{V}_{\mathcal{N}_T}} \sum_{(i,j) \in \mathcal{V}_{mn} \cap \mathcal{N}_T} \varphi_{\alpha}(y_{mn} - x_{ij}) \right), \end{aligned} \quad (1)$$

where φ_α is an edge-preserving potential function, β is a regularization parameter, \mathcal{V}_{ij} denotes the four closest neighbors of (i, j) not including (i, j) , and $\mathcal{V}_{\mathcal{N}_T} = \left(\bigcup_{(i,j) \in \mathcal{N}_T} \mathcal{V}_{ij} \right) \setminus \mathcal{N}_T$. Also we let $\hat{x}_{ij} = y_{ij}$ for $(i, j) \notin \mathcal{N}_T$. The minimizer $\hat{\mathbf{x}}$ of (1), which is the restored image, is found by Algorithm A which will be given later.

As mentioned in [18], in order for the minimization method in Step 3 above to be convergent, the function φ_α should satisfy (i) $\varphi_\alpha \in \mathcal{C}^1$, and (ii) φ_α is strongly convex on any bounded intervals. Examples of edge-preserving functions φ_α that satisfy these requirements are:

$$\varphi_\alpha(t) = |t|^\alpha, \quad 1 < \alpha \leq 2, \quad (2)$$

$$\varphi_\alpha(t) = 1 + \frac{|t|}{\alpha} - \log\left(1 + \frac{|t|}{\alpha}\right), \quad \alpha > 0, \quad (3)$$

$$\varphi_\alpha(t) = \log\left(\cosh\left(\frac{t}{\alpha}\right)\right), \quad \alpha > 0, \quad (4)$$

$$\varphi_\alpha(t) = \sqrt{\alpha + t^2}, \quad \alpha > 0, \quad (5)$$

see [10, 4, 5, 3, 8].

2.2 Cleaning random-valued noise

To clean the random-valued noise, an iterative two-phase scheme is proposed in [7]. The first phase is to use the adaptive center-weighted median filter (ACWMF) [9] to identify the noise candidates. Then the second phase is to restore those noise candidates by the same variational method proposed in [7]. These two phases are applied iteratively to the image. The basic idea of the method is that at the early iterations, we increase the thresholds in ACWMF so that it will only select pixels that are most likely to be noisy; and then they will be restored by the variational method. In the later iterations, the thresholds are decreased to include more noise candidates. The algorithm is as follows:

Algorithm II

1. Set $r = 0$. Initialize $\mathbf{y}^{(r)}$ to be the observed image \mathbf{y} .
2. Apply ACWMF with the thresholds $T_k^{(r)}$ to the image $\mathbf{y}^{(r)}$ to get the noise candidate set $\mathcal{M}^{(r)}$.
3. Let $\mathcal{N}^{(r)} = \bigcup_{l=0}^r \mathcal{M}^{(l)}$.
4. We restore all pixels in $\mathcal{N}^{(r)}$ by minimizing the same objective functional $F_{\mathbf{y}}$ in (1) over $\mathcal{N}^{(r)}$. The corresponding minimizer $\hat{\mathbf{x}}$ will be denoted by $\mathbf{y}^{(r+1)}$. Again the minimizer will be found by Algorithm A given below.
5. If $r \leq r_{\max}$, set $r = r+1$ and go back to Step 2. Otherwise, output the restored image $\hat{\mathbf{x}} = \mathbf{y}^{(r_{\max}+1)}$.

In Step 2, the thresholds are of the form

$$T_k^{(r)} = s \cdot \text{MAD}^{(r)} + \delta_k + 20(r_{\max} - r),$$

for $0 \leq k \leq 3$, $0 \leq r \leq r_{\max}$, and $0 \leq s \leq 0.6$. Here $[\delta_0, \delta_1, \delta_2, \delta_3] = [40, 25, 10, 5]$, and the robust estimate MAD denotes the “median of the absolute deviations from the median”, see [11, 2], i.e.

$$\text{MAD}^{(r)} = \text{median} \left\{ |y_{i-u, j-v}^{(r)} - \tilde{y}_{ij}^{(r)}| : -h \leq u, v \leq h \right\}$$

and

$$\tilde{y}_{ij}^{(r)} = \text{median} \left\{ y_{i-u, j-v}^{(r)} : -h \leq u, v \leq h \right\},$$

where $(2h + 1)$ defines the window length. In practice, $r_{\max} = 3$ is enough for satisfactory results.

The minimization algorithm in Step 3 of Algorithm I and in Step 4 of Algorithm II is given in [18]. It is a Jacobi-type relaxation algorithm and works on the residual $\mathbf{z} = \mathbf{x} - \mathbf{y}$. For convenience, let \mathcal{P} be \mathcal{N}_T in Step 3 of Algorithm I or $\mathcal{N}^{(r)}$ in Step 4 of Algorithm II. We restate the minimization algorithm in [18] as follows.

Algorithm A (Minimization Scheme)

1. Initialize $z_{ij}^{(0)} = 0$ for each (i, j) in the noise candidate set \mathcal{P} .

2. At each iteration k , do the following for each $(i, j) \in \mathcal{P}$:

(a) Calculate

$$\xi_{ij}^{(k)} = \beta \sum_{(m,n) \in \mathcal{V}_{ij}} \varphi'_\alpha(y_{ij} - z_{mn} - y_{mn}),$$

where z_{mn} , for $(m, n) \in \mathcal{V}_{ij}$, are the latest updates and φ'_α is the derivative of φ_α .

(b) If $|\xi_{ij}^{(k)}| \leq 1$, set $z_{ij}^{(k)} = 0$. Otherwise, find $z_{ij}^{(k)}$ by solving the nonlinear equation

$$\beta \sum_{(m,n) \in \mathcal{V}_{ij}} \varphi'_\alpha(z_{ij}^{(k)} + y_{ij} - z_{mn} - y_{mn}) = \text{sgn}(\xi_{ij}^{(k)}). \quad (6)$$

3. Stop the iteration when

$$\max_{i,j} \{|z_{ij}^{(k+1)} - z_{ij}^{(k)}|\} \leq \tau_A \quad \text{and} \quad \frac{F_{\mathbf{y}}(\mathbf{y} + \mathbf{z}^{(k)}) - F_{\mathbf{y}}(\mathbf{y} + \mathbf{z}^{(k+1)})}{F_{\mathbf{y}}(\mathbf{y} + \mathbf{z}^{(k)})} \leq \tau_A,$$

where τ_A is some given tolerance.

It was shown in [18] that the solution $z_{ij}^{(k)}$ of (6) satisfies

$$\text{sgn}(z_{ij}^{(k)}) = -\text{sgn}(\xi_{ij}^{(k)}), \quad (7)$$

and that $\mathbf{z}^{(k)}$ converges to $\hat{\mathbf{z}} = \hat{\mathbf{x}} - \mathbf{y}$ where $\hat{\mathbf{x}}$ is the minimizer for (1).

3 Algorithm for Solving (6)

It is well-known that the edges and details are preserved better if the potential function $\varphi_\alpha(t)$ is close to $|t|$ —the celebrated TV norm function developed in [21]. For φ_α in (2), this means that α should be chosen close to 1. For φ_α in (3)–(5), we should choose α close to 0. Notice that all φ'_α will have a steep increase near zero and that φ''_α will have a large value at zero—in fact it is infinite for φ_α in (2). The function (6) therefore will have very large slopes in some regions which makes the minimization difficult. Although Newton’s minimization is preferable to speed up the convergence, its use is delicate since the convergence domain can be very narrow. In this section we discuss how to find the initial guess such that Newton’s method is guaranteed to converge. We will focus on how to solve (6) when $\varphi_\alpha(t) = |t|^\alpha$ with $\alpha > 1$. With some modifications, similar techniques can be applied to other edge-preserving φ_α too.

According to Step 2(b) of Algorithm A, we only need to solve (6) if $|\xi_{ij}^{(k)}| > 1$. We first consider the case where $\xi_{ij}^{(k)} > 1$. When solving (6), $z_{mn} + y_{mn} - y_{ij}$, for $(m, n) \in \mathcal{V}_{ij}$, are known values. Let these values be denoted by d_j , for $1 \leq j \leq 4$, and be arranged in an increasing order: $d_j \leq d_{j+1}$. Then (6) can be rewritten as

$$H(z) \equiv -1 + \alpha \beta \sum_{j=1}^4 \text{sgn}(z - d_j) |z - d_j|^{\alpha-1} = 0. \quad (8)$$

Since each term inside the summation sign above is a strictly increasing function on \mathbb{R} , $H(z)$ is a strictly increasing function on \mathbb{R} . Clearly $H(d_1) < 0$ and $\lim_{z \rightarrow \infty} H(z) = \infty$. Hence (8) has a unique solution $z^* > d_1$. By evaluating $\{H(d_j)\}_{j=2}^4$, we can check that if any one of the d_j , $2 \leq j \leq 4$, is the root z^* . If not, then z^* lies in one of the following intervals:

$$(d_1, d_2), (d_2, d_3), (d_3, d_4), \text{ or } (d_4, \infty), \quad (9)$$

We first consider the case where z^* is in one of the finite intervals (d_j, d_{j+1}) . For simplicity, we give the details only for the case where $z^* \in (d_2, d_3)$. The other cases can be analyzed similarly.

Let $z^* \in (d_2, d_3)$, i.e. $H(d_2) < 0$ and $H(d_3) > 0$. Then we compute $H\left(\frac{d_2+d_3}{2}\right)$. Without loss of generality, let us assume that $H\left(\frac{d_2+d_3}{2}\right) > 0$. Our aim is to find an initial guess $z^{(0)} \in [d_2, (d_2 + d_3)/2]$ with $H(z^{(0)}) \leq 0$. Unfortunately, we cannot use d_2 as the initial guess as $H'(d_2)$ is undefined. We will prove in Theorem 2 that Newton's method with $z^{(0)} \equiv d_2 + \varepsilon$ can solve (8), where $\varepsilon > 0$ is given below.

Lemma 1. *Let*

$$\varepsilon \equiv \left[\frac{-H(d_2)}{4\alpha\beta} \right]^{\frac{1}{\alpha-1}}. \quad (10)$$

Then $H(d_2 + \varepsilon) \leq 0$. As a result, $z^ \in [d_2 + \varepsilon, (d_2 + d_3)/2]$.*

Proof. First let $\tilde{\varepsilon} = \min\{(d_3 - d_2)/2, \varepsilon\} > 0$. By (8), we have

$$H(d_2 + \tilde{\varepsilon}) = -1 + \alpha\beta \left[(d_2 - d_1 + \tilde{\varepsilon})^{\alpha-1} + \tilde{\varepsilon}^{\alpha-1} - (d_3 - d_2 - \tilde{\varepsilon})^{\alpha-1} - (d_4 - d_2 - \tilde{\varepsilon})^{\alpha-1} \right].$$

For $1 < \alpha \leq 2$, we can easily verify the inequalities:

$$\begin{aligned} (c + \delta)^{\alpha-1} &\leq c^{\alpha-1} + \delta^{\alpha-1}, \quad \text{for all } c, \delta \geq 0, \\ (c - \delta)^{\alpha-1} &\geq c^{\alpha-1} - \delta^{\alpha-1}, \quad \text{for all } c \geq \delta \geq 0. \end{aligned}$$

Since $\tilde{\varepsilon} \leq (d_3 - d_2)/2 < (d_3 - d_2) \leq (d_4 - d_2)$, we obtain

$$\begin{aligned} H(d_2 + \tilde{\varepsilon}) &\leq -1 + \alpha\beta \left\{ (d_2 - d_1)^{\alpha-1} + \tilde{\varepsilon}^{\alpha-1} + \tilde{\varepsilon}^{\alpha-1} - [(d_3 - d_2)^{\alpha-1} - \tilde{\varepsilon}^{\alpha-1}] - [(d_4 - d_2)^{\alpha-1} - \tilde{\varepsilon}^{\alpha-1}] \right\} \\ &= H(d_2) + 4\alpha\beta\tilde{\varepsilon}^{\alpha-1}. \end{aligned}$$

By (10), we have

$$H(d_2 + \tilde{\varepsilon}) \leq H(d_2) + 4\alpha\beta\tilde{\varepsilon}^{\alpha-1} \leq H(d_2) + 4\alpha\beta\varepsilon^{\alpha-1} = 0.$$

However, because $H((d_2 + d_3)/2) > 0$ and H is strictly increasing, we must have $\tilde{\varepsilon} < (d_3 - d_2)/2$. As a result, $\tilde{\varepsilon} = \varepsilon$ and $H(d_2 + \varepsilon) \leq 0$. \square

Theorem 2. *Let $z^{(0)} = d_2 + \varepsilon$ be the initial guess where ε is defined in (10). Then the sequence generated by Newton's method, i.e.*

$$z^{(n+1)} = z^{(n)} - \frac{H(z^{(n)})}{H'(z^{(n)})}, \quad (11)$$

converges to the root z^ of $H(z)$.*

Proof. Consider the Taylor expansion of $H(z)$ at $z = z^*$. We have

$$H(z) = H(z^*) + (z - z^*)H'(\tilde{z}) = (z - z^*)H'(\tilde{z}),$$

where \tilde{z} lies strictly between z and z^* . Hence by (11),

$$z^* - z^{(n+1)} = \left(1 - \frac{H'(\tilde{z}^{(n)})}{H'(z^{(n)})}\right) (z^* - z^{(n)}), \quad (12)$$

where $\tilde{z}^{(n)}$ lies strictly between $z^{(n)}$ and z^* . We note that $d_2 < z^{(0)} < \tilde{z}^{(0)} < z^* < (d_2 + d_3)/2$.

We need the following facts to complete the proof:

- F1. Clearly from the definition (8), $H'(z) = \alpha(\alpha-1)\beta \sum_{j=1}^4 |z - d_j|^{\alpha-2} > 0$ for all $z \in (d_2, d_3)$.
- F2. Since $H'''(z) = \alpha(\alpha-1)(\alpha-2)(\alpha-3)\beta \sum_{j=1}^4 |z - d_j|^{\alpha-4} > 0$ for all $z \in (d_2, d_3)$, $H''(z)$ is strictly increasing in (d_2, d_3) .
- F3. Define $W(z) \equiv \alpha(\alpha-1)\beta \sum_{j=2}^3 |z - d_j|^{\alpha-2}$. Clearly $W(z) < H'(z)$ for all z . Moreover, $W'(z) < 0$ for $z \in (d_2, (d_2 + d_3)/2)$. Hence $W(z)$ is a strictly decreasing function in $(d_2, (d_2 + d_3)/2)$.

We divide the convergence proof in two cases:

- (i) $H''(z^*) \leq 0$: F2 implies that $H''(z) < 0$ in (d_2, z^*) . Hence $H'(z)$ is decreasing in (d_2, z^*) . Therefore, $H'(\tilde{z}) \leq H'(z)$ for $d_2 < z < \tilde{z} < z^*$. Together with F1, we have

$$0 \leq 1 - \frac{H'(\tilde{z})}{H'(z)} < 1, \quad \text{for all } d_2 < z < \tilde{z} < z^*.$$

Therefore, from (12), we have

$$0 \leq z^* - z^{(n+1)} < z^* - z^{(n)}, \quad n = 0, 1, \dots,$$

i.e. the sequence $\{z^{(n)}\}$ converges monotonically to z^* from the left.

- (ii) $H''(z^*) > 0$: For all $z \in (d_2, (d_2 + d_3)/2)$, since

$$|z - d_1|^{\alpha-2} \leq |z - d_2|^{\alpha-2} \quad \text{and} \quad |z - d_4|^{\alpha-2} \leq |z - d_3|^{\alpha-2},$$

we have

$$H'(z) \leq 2\alpha(\alpha-1)\beta \sum_{j=2}^3 |z - d_j|^{\alpha-2} = 2W(z), \quad \text{for all } z \in (d_2, (d_2 + d_3)/2).$$

Here $W(z)$ is defined in F3. Since $W(z)$ is a strictly decreasing function in $(d_2, (d_2 + d_3)/2)$ and $W(z) < H'(z)$ for all z , we have

$$H'(\tilde{z}) \leq 2W(\tilde{z}) \leq 2W(z) < 2H'(z), \quad \text{for all } d_2 < z < \tilde{z} < z^*.$$

Hence

$$\left| 1 - \frac{H'(\tilde{z})}{H'(z)} \right| < 1, \quad \text{for all } d_2 < z < \tilde{z} < z^*.$$

Therefore by (12), as long as $d_2 < z^{(n)} < z^*$, we have

$$|z^* - z^{(n+1)}| < |z^* - z^{(n)}|,$$

i.e. the sequence $\{z^{(n)}\}$ converges to z^* as long as $z^{(n)} < z^*$ for all n .

But what if after some iterations, $z^{(m)} > z^*$? Since $H''(z^*) > 0$, by F2, we have $H''(z) > 0$ in $[z^*, d_3]$. This implies that $H'(z)$ is increasing in $[z^*, d_3]$. As a result, $H'(\tilde{z}) \leq H'(z)$ for all $z^* < \tilde{z} < z$. Therefore,

$$0 \leq 1 - \frac{H'(\tilde{z})}{H'(z)} < 1, \quad \text{for all } z^* < \tilde{z} < z.$$

Hence, from (12), we have

$$0 \leq z^{(n+1)} - z^* < z^{(n)} - z^*, \quad n = m, m+1, \dots,$$

i.e. the sequence $\{z^{(n)}\}_{n=m}^\infty$ converges monotonically to z^* from the right.

□

This finishes the proof for the case when $H\left(\frac{d_2+d_3}{2}\right) > 0$. If $H\left(\frac{d_2+d_3}{2}\right) < 0$, then we locate $z^{(0)} \in ((d_2 + d_3)/2, d_3]$. More precisely, $z^{(0)} = d_3 - \varepsilon$ with $\varepsilon = [H(d_3)/(4\alpha\beta)]^{\frac{1}{\alpha-1}}$. The rest of the proof will be similar.

The same result holds when z^* lies in other finite intervals (d_j, d_{j+1}) , $j = 1, 2, 3$. If $H(d_4) < 0$, this means $z^* \in (d_4, \infty)$. Since

$$H''(z) = \alpha(\alpha-1)(\alpha-2)\beta \sum_{j=1}^4 \operatorname{sgn}(z-d_j)|z-d_j|^{\alpha-3} < 0, \quad \text{for all } z \in (d_4, \infty),$$

we are in a situation similar to case (i) in Theorem 2. In fact, as $H'(z)$ is strictly decreasing in (d_4, ∞) , $0 < 1 - H'(\tilde{z})/H(z) < 1$ for all $d_4 < z < \tilde{z} < z^*$. Therefore it suffice to choose an initial guess $z^{(0)} = d_4 + \varepsilon$ such that $H(z^{(0)}) < 0$. (Again we cannot choose $z^{(0)} = d_4$ as $H'(d_4)$ is undefined.) Similar to Lemma 1, we can choose $\varepsilon = [-H(d_4)/(4\alpha\beta)]^{\frac{1}{\alpha-1}}$. Then one can show from (12) that $0 \leq z^* - z^{(n+1)} < z^* - z^{(n)}$, for $n = 0, 1, \dots$, i.e. $\{z^{(n)}\}$ converges monotonically to z^* from the left.

We remark that since we are considering the case that $\xi_{ij}^{(k)} > 1$, by (7), $\operatorname{sgn}(z^*) = -\operatorname{sgn}(\xi_{ij}^{(k)}) = -1$. Hence $z^* < 0$. Thus we may not need to check all the intervals in (9) for z^* . In fact, if $d_\ell < 0 < d_{\ell+1}$, then we only have to check the intervals $\{(d_j, d_{j+1})\}_{j=1}^\ell$. This can simplify the algorithm (see Step 1 in Algorithm B below).

Finally, we turn to the case where $\xi_{ij}^{(k)} < -1$. The nonlinear equation in (8) becomes:

$$1 + \alpha\beta \sum_{j=1}^4 \operatorname{sgn}(z-d_j)|z-d_j|^{\alpha-1} = 0,$$

where the left-hand-side function is still a strictly increasing function in z , and that $z^* > 0$ by (7). The convergence proof is almost the same with minor modifications.

We summarize the results into the following algorithm. It works for both $\xi_{ij}^{(k)} > 1$ and $\xi_{ij}^{(k)} < -1$.

Algorithm B (Newton's Solver for Solving (6))

1. Check the signs of $H(d_j)$, $1 \leq j \leq 4$. (One may not need to check all four points by taking into account the sign of z^* using (7).)
2. If $H(d_1) > 0$ or $H(d_4) < 0$, let

$$z^{(0)} = \begin{cases} d_1 - \left\{ \frac{H(d_1)}{4\alpha\beta} \right\}^{\frac{1}{\alpha-1}}, & \text{if } H(d_1) > 0, \\ d_4 + \left\{ -\frac{H(d_4)}{4\alpha\beta} \right\}^{\frac{1}{\alpha-1}}, & \text{if } H(d_4) < 0. \end{cases}$$

3. Else locate the interval (d_j, d_{j+1}) which contains the root z^* , and let

$$z^{(0)} = \begin{cases} d_{j+1} - \left\{ \frac{H(d_{j+1})}{4\alpha\beta} \right\}^{\frac{1}{\alpha-1}}, & \text{if } H\left(\frac{d_j + d_{j+1}}{2}\right) < 0, \\ d_j + \left\{ -\frac{H(d_j)}{4\alpha\beta} \right\}^{\frac{1}{\alpha-1}}, & \text{if } H\left(\frac{d_j + d_{j+1}}{2}\right) > 0. \end{cases}$$

4. Apply Newton's method to obtain z^* up to a given tolerance τ_B .

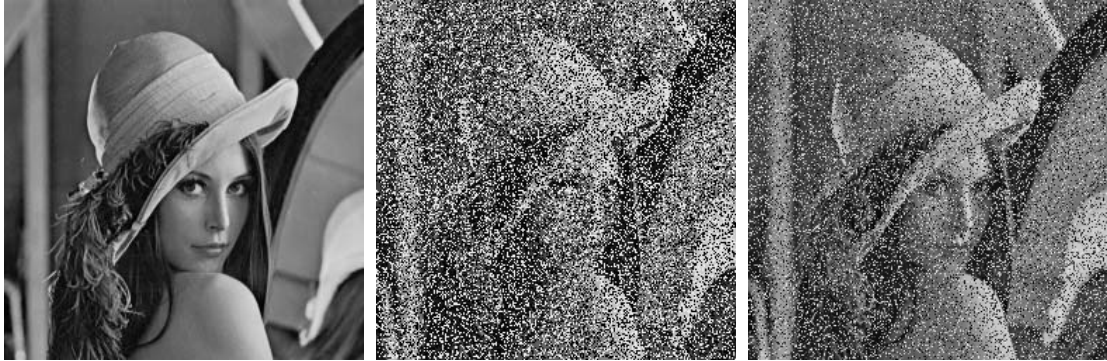


Figure 1: (Left) The original Lena image. (Middle) The noisy image corrupted with 50% salt-and-pepper noise. (Right) The noisy image corrupted with 40% random-valued noise.

α	inner iterations	outer iterations	α	inner iterations	outer iterations
1.3	5	117	1.3	5	319
1.2	6	201	1.2	6	512
1.1	9	290	1.1	9	1208

Table 1: The number of iterations in restoring noisy image corrupted by (left) salt-and-pepper noise and (right) random-valued noise.

4 Numerical Results

In this section, we stimulate the restoration of the 256-by-256 gray scale image *Lena* corrupted by 50% salt-and-pepper noise and 40% random-valued impulse noise with dynamic range $[0, 255]$, see Figure 1. Here the salt noise (i.e. s_{\max}) and the pepper noise (i.e. s_{\min}) are of equal probability and the random-valued noise are uniformly distributed in the dynamic range. We clean the salt-and-pepper noise by Algorithm I with threshold $T = 5$ and the random-valued noise by Algorithm II with $s = 0.1$. In both algorithms, we use windows of size 9-by-9 for noise detection.

We test our Newton's method with different magnitudes of α and choose $\beta = 2$ for all settings. The tolerances in Algorithms A and B are chosen to be $\tau_A = (s_{\max} - s_{\min}) \times 10^{-4}$ and $\tau_B = 5 \times 10^{-4}$ respectively. In Table 1, we give, for different values of α , the maximum number of inner iterations (i.e. maximum number of Newton's iterations in Step 4 of Algorithm B), and the total number of outer iterations (i.e. maximum k in Algorithm A).

From the table, we see that around 5 to 9 iterations are sufficient for Newton's method to converge. The smaller α is, the more iterations $|t|^\alpha$ requires. But in practice, there will be stair-case effects in the restored image if α is too small. To restore the best image, $1.25 \leq \alpha \leq 1.40$ is sufficient. We give the restored images in Figure 2. We see that the noise are successfully suppressed while the edges and details are well preserved.

5 Conclusions

In this report, we first give an overview of denoising schemes for cleaning salt-and-pepper and random-valued impulse noise. Experimental results show that the images are restored satisfactory even at very high noise level. Then we present an algorithm for solving the variational equations resulting from the denoising schemes. It is the essential step in the restoration process. To overcome the difficulty in finding the convergence domain, we have derived a formula for the initial guess; and proved that with it, Newton's method is guaranteed to converge.



Figure 2: (Left) Restoration from image corrupted by salt-and-pepper noise using $\alpha = 1.3$ and $\beta = 2.5$. (Right) Restoration from image corrupted by random-valued noise using $\alpha = 1.3$ and $\beta = 2.3$.

References

- [1] G. R. Arce and R. E. Foster, “Detail-preserving ranked-order based filters for image processing,” *IEEE Transactions on Acoustics, Speech, and Signal Processing*, 37 (1989), pp. 83–98.
- [2] J. Astola and P. Kuosmanen, *Fundamentals of Nonlinear Digital Filtering*. Boca Raton, CRC, 1997.
- [3] M. Black and A. Rangarajan, “On the unification of line processes, outlier rejection, and robust statistics with applications to early vision,” *International Journal of Computer Vision*, 19 (1996), pp. 57–91.
- [4] C. Bouman and K. Sauer, “A generalized Gaussian image model for edge-preserving MAP estimation,” *IEEE Transactions on Image Processing*, 2 (1993), pp. 296–310.
- [5] C. Bouman and K. Sauer, “On discontinuity-adaptive smoothness priors in computer vision,” *IEEE Transactions on Pattern Analysis and Machine Intelligence*, 17 (1995), pp. 576–586.
- [6] R. H. Chan, C.-W. Ho, and M. Nikolova, “Impulse noise removal by median-type noise detectors and edge-preserving regularization,” *Report*, Department of Mathematics, The Chinese University of Hong Kong, 2003-28 (302).
- [7] R. H. Chan, C. Hu, and M. Nikolova, “An iterative procedure for removing random-valued impulse noise,” *Report*, Department of Mathematics, The Chinese University of Hong Kong, 2003-33 (307).
- [8] P. Charbonnier, L. Blanc-Féraud, G. Aubert, and M. Barlaud, “Deterministic edge-preserving regularization in computed imaging,” *IEEE Transactions on Image Processing*, 6 (1997), pp. 298–311.
- [9] T. Chen and H. R. Wu, “Space variant median filters for the restoration of impulse noise corrupted images,” *IEEE Transactions on Circuits and Systems II*, 48 (2001), pp. 784–789.
- [10] P. J. Green, “Bayesian reconstructions from emission tomography data using a modified EM algorithm,” *IEEE Transactions on Medical Imaging*, MI-9 (1990), pp. 84–93.
- [11] F. R. Hampel, E. M. Ronchetti, P. J. Rousseeuw, and W. A. Stahel, *Robust statistics: The Approach based on influence functions*, New York: Wiley, 1986.
- [12] W.-Y. Han and J.-C. Lin, “Minimum-maximum exclusive mean (MMEM) filter to remove impulse noise from highly corrupted images,” *Electronics Letters*, 33 (1997), pp. 124–125.
- [13] R. C. Hardie and K. E. Barner, “Rank conditioned rank selection filters for signal restoration,” *IEEE Transactions on Image Processing*, 3 (1994), pp. 192–206.

- [14] T. S. Huang, G. J. Yang, and G. Y. Tang, “Fast two-dimensional median filtering algorithm,” *IEEE Transactions on Acoustics, Speech, and Signal Processing*, 1 (1979), pp. 13–18.
- [15] H. Hwang and R. A. Haddad, “Adaptive median filters: new algorithms and results,” *IEEE Transactions on Image Processing*, 4 (1995), pp. 499–502.
- [16] S.-J. Ko and Y. H. Lee, “Center weighted median filters and their applications to image enhancement,” *IEEE Transactions on Circuits and Systems*, 38 (1991), pp. 984–993.
- [17] Y. H. Lee and S. A. Kassam, “Generalized median filtering and related nonlinear filtering techniques,” *IEEE Transactions on Acoustics, Speech, and Signal Processing*, 33 (1985), pp. 672–683.
- [18] M. Nikolova, “A variational approach to remove outliers and impulse noise,” to appear in *Journal of Mathematical Imaging and Vision*, vol. 20, n. 1/2 (Jan. 2004).
- [19] I. Pitas and A. Venetsanopoulos, “Nonlinear mean filters in image processing,” *IEEE Transactions on Acoustics, Speech, and Signal Processing*, 34 (1986), pp. 600–609.
- [20] G. Pok, J.-C. Liu, and A. S. Nair, “Selective removal of impulse noise based on homogeneity level information,” *IEEE Transactions on Image Processing*, 12 (2003), pp. 85–92.
- [21] L. Rudin, S. Osher, and E. Fatemi, “Nonlinear total variation based noise removal algorithms,” *Physica D*, 60 (1992), pp. 259–268.
- [22] T. Sun and Y. Neuvo, “Detail-preserving median based filters in image processing,” *Pattern Recognition Letters*, 15 (1994), pp. 341–347.